Journal of Materials Chemistry A

ROYAL SOCIETY OF CHEMISTRY

PAPER

View Article Online
View Journal | View Issue



Cite this: J. Mater. Chem. A, 2023, 11, 10850

# Laccase-catalyzed functionalization of phenol-modified carbon nanotubes: from grafting of metallopolyphenols to enzyme self-immobilization†

Umberto Contaldo,[a] Solène Gentil,[ab] Elise Courvoisier-Dezord,[c] Pierre Rousselot-Pailley,[c] Fabrice Thomas,[a] Thierry Tron *[c] and Alan Le Goff *[a]

Received 13th February 2023
Accepted 14th April 2023

DOI: 10.1039/d3ta00849e

rsc.li/materials-a

We report the unprecedented use of laccase to functionalize phenol-modified carbon nanotubes (CNTs). Enzymatically-generated metallopolyphenols or the laccase itself can be mildly and efficiently immobilized using the ability of laccase to generate phenoxyl radicals. Electrochemistry, XPS and EPR spectroscopy were used to assess the enzyme-catalyzed CNT functionalization. The efficient immobilization of laccase is confirmed by the high direct bioelectrocatalytic reduction of oxygen with a maximum current density of 1.95 mA $cm^{-2}$.



## Introduction

Laccases are copper-containing oxidases which have been extensively studied both for their ability to oxidize a wide variety of substrates and for their concomitant ability to reduce $O_2$ into water at high redox potentials. A type 1 (T1) mononuclear copper centre, located near the surface of the protein, is responsible for outer-sphere oxidation of substrates, while a trinuclear copper centre (TNC) is responsible for the concomitant reduction of the laccase co-substrate, dioxygen. Many laccase-based biotechnological applications rely on these exceptional properties.[1–6] Their ability to generate phenoxy radicals from the oxidation of phenols has been especially employed in polymerization and cross-linking processes.[5–8] Tyrosine-containing macromolecules such as peptides[9] and proteins[10] can be enzymatically cross-linked under mild conditions thanks to laccase-catalyzed generation of phenoxy radicals. Laccases have also been employed in electrochemical applications, mostly biosensors and biofuel cells, relying on the efficient immobilization and electrical wiring of laccases at the electrode surface.[3,4,11–15] LAC3 is a typical fungal laccase which can be obtained with high yield as recombinant protein in yeast.[16,17] We have already exploited its excellent versatility and performances in several applications.[18–23] While many strategies can be applied to immobilize these enzymes at electrodes,[24–28] electrografting of aryldiazonium salts[29–31] has proven to provide a reliable way of introducing functional groups at electrode surfaces for post-functionalization with enzymes. We and others have taken advantages of several types of aryldiazonium salts to graft laccases using different types of selective covalent binding reactions such as Huisgen cycloaddition,[18] oxime ligation[32] or imino/amide binding.[33] This has been particularly the case in the construction of carbon nanotube (CNT)-based electrodes. CNTs provide a unique combination of biocompatibility, high conductivity and high surface area. Furthermore, the functionalization of CNTs by many covalent and non-covalent techniques has extended their exceptional properties to the immobilization of small molecules as well as macromolecules, providing hybrid nanomaterials for many applications. Functionalization of CNTs often requires specific harsh conditions to efficiently attack and modify the pi-conjugated network of CNT sidewalls.[34,35] This is particularly the case when modifying CNTs with macromolecules such as enzymes or polymers to design nanocomposites. In this respect the design of "grafting from" techniques has provided a mild method to modify CNTs by first introducing an initiator at the surface of CNTs, followed by the polymerisation of the monomer in solution from this seed layer.[36] These have been notably developed using diazonium chemistry and atom transfer radical polymerisation (ATRP).[37,38] The main advantage of this technique resides in providing high grafting density while preventing additional diffusion limitations when macromolecules have to be grafted by a "grafting onto" method. On the other hand, enzymes are potentially offering mild, aqueous and green-chemistry-based conditions for the modification of CNT sidewalls. A few examples already describe the use of peroxidases and xanthine oxidases to degrade CNTs.[39–45] In particular,

[a]Univ. Grenoble Alpes, CNRS, DCM, 38000 Grenoble, France. E-mail: alan.le-goff@univ-grenoble-alpes.fr

[b]Univ. Grenoble Alpes, CEA, CNRS, BIG-LCBM, 38000 Grenoble, France

[c]Aix Marseille Université, Centrale Marseille, CNRS, iSm2 UMR 7313, 13397 Marseille, France. E-mail: thierry.tron@univ-amu.fr

† Electronic supplementary information (ESI) available. See DOI: https://doi.org/10.1039/d3ta00849e

A. Bianco and colleagues have shown that catechol-modified CNTs enhance peroxidase activity increasing CNT enzymatic degradation.[41]

In this work, we investigated the grafting of laccase and 4-ferrocenylphenol (FcPhOH) on CNTs using laccase as the polymerization catalyst. CNTs were first modified by electrografting of 4-hydroxybenzenediazonium salt. This polyphenylenephenol layer was then employed as a seed layer for grafting poly[ferrocenylphenol]. This strategy represents an unprecedented attempt to use an enzyme to catalyse the mild "grafting to" functionalization of CNTs by a metallopolymer. Furthermore, using the well-known ability of laccases to cross-link proteins and peptides through the oxidation of tyrosine, the laccase itself was auto-catalytically immobilized at these polyphenylenephenol-modified CNTs. Thus immobilized, the enzyme exhibits a direct electron transfer (DET) with the CNTs allowing an efficient bioelectrocatalytic oxygen reduction.

## Results and discussion

### Reactivity of laccase with 4-ferrocenylphenol

FcPhOH was synthesized using a procedure modified from a previously-described procedure.[46] FcPhOH was chosen as a redox probe bearing a non-protected phenol, a classic substrate for laccase. Reactivity of laccase with FcPhOH was first investigated by UV-visible spectroscopy (Fig. 1).

As laccase was added to a solution of FcPhOH in acetate buffer pH 5.5 (in the presence of 2% DMSO used to dissolve FcPhOH in the aqueous buffer), FcPhOH oxidation was monitored over time. In the first seconds of the addition, a bright yellow color confirmed the formation of an oxidation product. FcPhO$^{\bullet}$ radical (*i.e.* the putative oxidation product) appeared as an intense band at 350 nm in the absorption spectrum which then progressively disappeared over one hour. This is in line with the formation of phenoxyl radicals in solution and their subsequent polymerization.[47] After several hours, a bleaching of the solution was observed, accompanied by the formation of an orange precipitate. After filtration, this precipitate was analyzed by MALDI-TOF MS (Fig. 1C). A series of peaks separated by a mass of 276 g mol$^{-1}$ was observed in the spectrum. This is consistent with the presence of oligomers of the poly-oxyphenylene derivative, poly-[FcPhO], of FcPhOH. Oligomers of $n = 3$ to 7, the structure of which is supported by their isotopic composition (see inset, Fig. 1B) are unambiguously observed in the $m/z$ profile.

The reactivity of laccase with FcPhOH was next investigated by electrochemistry (Fig. 2).

First, the CV recorded for a 0.25 mM solution (0.1 M acetate buffer, pH 5.5, 25% DMSO) displays one reversible system at $E_{1/2}^{ox1} = 0.24$ V *vs.* SCE corresponding to the typical monoelectronic Fc/Fc$^+$ oxidation and one irreversible system at $E_p^{ox2} = 0.67$ V *vs.* SCE corresponding to the oxidation of phenol. In the presence of laccase (4 μM), an irreversible system is observed at the redox potential of the Fc/Fc$^+$ couple in an oxygen-saturated solution. This corresponds to the mediated reduction of $O_2$ by laccase. It is important to note that this irreversible catalytic wave decreases upon further scanning. This is caused by the polymerization of

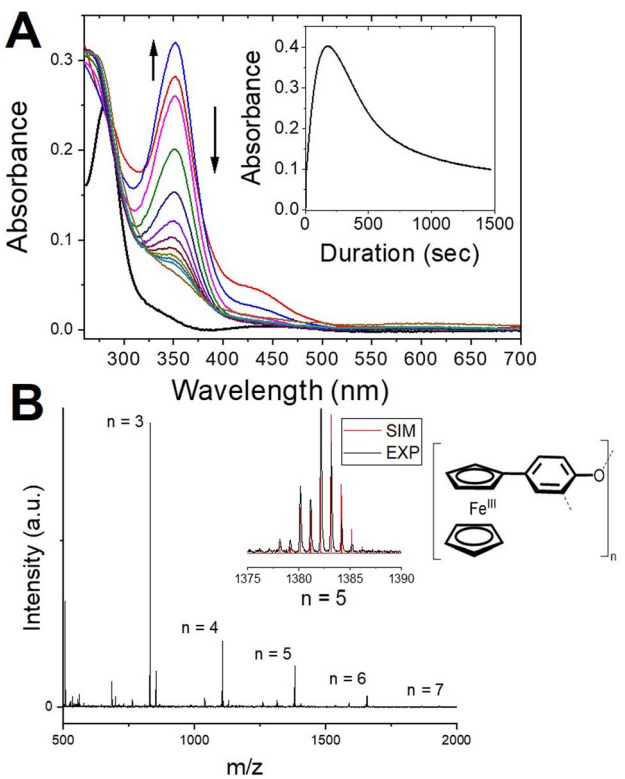


Fig. 1 (A) Absorption spectra of a 20 μM solution of FcPhOH in 0.1 M acetate buffer pH 5.5 (2% DMSO) before ($t = 0$) and after addition of 3 μM laccase ($t = 2$, 5, 10, 20, 25, 35, 40, 50 and 90 min). A plot of the evolution of absorbance at $\lambda = 350$ nm *vs.* time is given in the inset; (B) MALDI-TOF MS profile of the orange precipitate formed after 24 h (inset: experimental and simulated isotopic profile for a $m/z$ corresponding to $n = 5$).

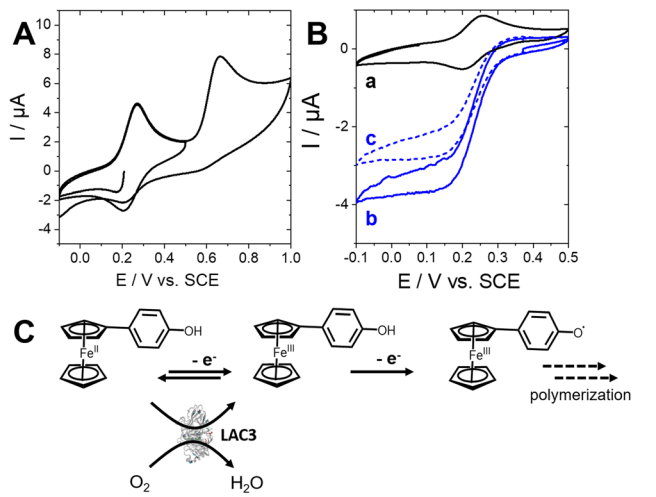


Fig. 2 (A) CV of a 0.25 mM solution of FcPhOH in 0.1 M acetate buffer pH 5.5 under Ar (25% DMSO, $v = 100$ mV s$^{-1}$); (B) CV of a 0.25 mM solution of FcPhOH in the presence of 4 μM laccase under (a) Ar and (b) under $O_2$ after one CV cycle and (c) after two CV cycles (25% DMSO, $v = 5$ mV s$^{-1}$, $\omega = 400$ rpm); (C) schematic representation of the electrochemical behaviour of FcPhOH.

FcPhOH in solution (as observed previously in the absorption spectra) which decreases the availability of FcPhOH in solution as the redox partner of laccase. This experiment not only illustrates the well-known ability of laccase to catalytically oxidize ferrocene while reducing $O_2$ but also confirms the ability of laccase to doubly oxidize FcPhOH into the corresponding 4-ferrocenylphenoxy radical $Fc^+PhO^\bullet$.

### Enzymatic grafting of poly[ferrocenylphenol] at the MWCNT electrode modified with 4-hydroxybenzenediazonium tetrafluoroborate

MWCNT electrodes were first modified with 4-hydroxybenzenediazonium tetrafluoroborate by electrografting.[48] Fig. 3A shows the typical CV observed in a 1 mM solution in MeCN–0.1 M TBAP.[11,49–51] An irreversible reduction is observed at $E_p^{red} = -0.095$ V *vs.* $Fc/Fc^+$ corresponding to the reduction of the diazonium and the generation of aryl radicals.

Subsequent CV scans are progressively shifted towards negative potentials, indicating the formation of a polyphenylenephenol layer at the surface of MWCNT sidewalls.[11,51,52] The EPR spectrum of a dispersion of phenol-modified MWCNTs in frozen water/DMSO (90/10) shows a sharp and isotropic resonance at $g = 2.002$ ($\Gamma = 0.5$ mT). This signal is attributed to magnetically isolated radical sites in the MWCNT structure, confirming the covalent modification of CNTs.[53] Then, these phenol-modified MWCNT electrodes were soaked for 30 min in 0.25 mM solution of FcPhOH in 0.1 M acetate buffer pH 5.5 (25% DMSO) in the presence of 4 μM laccase. After a thorough rinsing, the electrochemistry was performed in MeCN–0.1 M TBAP.

The system observed at 0.16 V *vs.* $Fc/Fc^+$ corresponds to the reversible oxidation of ferrocene. Note that when the electrode is soaked in a solution of FcPhOH without laccase, a negligible redox signal is observed (curve e, Fig. 4B). The $\Delta E = 20$ mV at slow scan rates is consistent with a surface-controlled redox process. Subsequent soakings of the electrode performed in fresh laccase/FcPhOH solutions lead to an increase of the intensity of the reversible system confirming the increase of the FcPhOH surface concentration. On the other hand, prolonging the soaking time do not significantly increases the ferrocene redox system. This is consistent with the fact that the grafting of the $Fc^+PhO^\bullet$ radicals at the phenol-modified surface of CNTs is likely more efficient at maximum concentration of radicals in solution (as observed in the absorbance spectra in Fig. 1A after 30 min) while the heterogeneous grafting further competes with the homogeneous polymerisation after prolonged soaking times. Integration of the charge reveals that maximum surface concentrations can reach values as high as 83 ± 8 nmol $cm^{-2}$. The linear dependence of the current against the square root of the scan rate (Fig. 4D) is consistent with a charge-diffusion limiting process in line with the immobilization of a metallopolymer.[54–56] The mechanism of this poly-$[Fc^+PhO]_n$ grafting on phenol-modified MWCNTs likely involves the reaction of $Fc^+PhO^\bullet$ radicals in the *ortho* position of the immobilized phenol. We investigated the generation of reactive phenoxy radicals during turnovers by EPR spectroscopy. However, our attempts to detect phenoxy radicals at the surface of MWCNT sidewalls directly by EPR were unsuccessful. Indeed, spectra are dominated by the signature of magnetically isolated radical sites in the MWCNT structure. This feature is identical in the presence or in the absence of the enzyme (Fig. 3B, spectra b and c). DMPO was also used in order to trap short-lived phenoxy radicals, without success. We interpret the absence of any detectable phenoxyl or DMPO adduct EPR signal as a potential consequence of a low density of enzymatically-generated phenoxy radicals at the CNT surface.

The surface of the modified MWCNT electrode was investigated by X-ray photoelectron spectroscopy (XPS, Fig. 5 and S1†). The

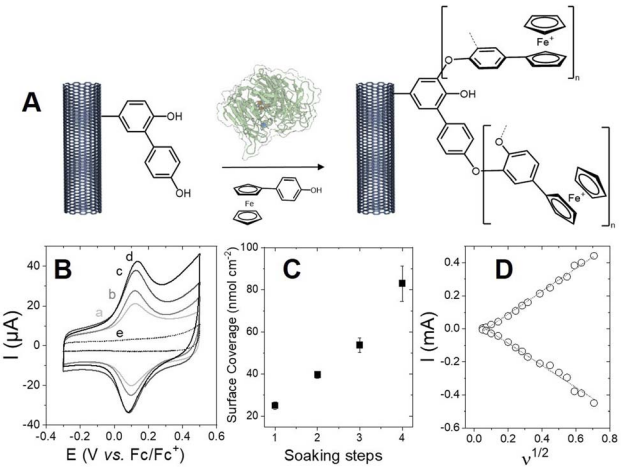


Fig. 4 (A) Schematic representation of the laccase-catalyzed functionalization of MWCNT electrodes with poly-$[Fc^+PhO]_n$; (B) CV of a phenol-functionalized MWCNT electrode after (a–d) consecutive soaking steps in a 0.25 mM solution of FcPhOH in 0.1 M acetate buffer pH 5.5 (25% DMSO) in the presence of 4 μM laccase and (e) in the absence of laccase ($v = 10$ mV $s^{-1}$, MeCN–0.1 M TBAP); (C) plot of the final ferrocene surface concentration against the number of soaking steps; (D) plot of the oxidation and reduction peak currents against the square root of the scan rate for a phenol-functionalized MWCNT electrode after 4 soaking steps in a 0.25 mM solution of FcPhOH in 0.1 M acetate buffer pH 5.5 (25% DMSO) in the presence of 4 μM laccase (MeCN–0.1 M TBAP).

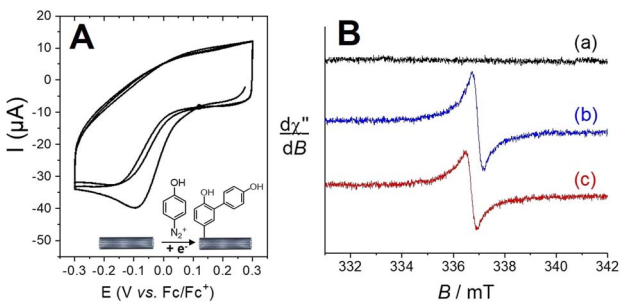


Fig. 3 (A) CV of a 1 mM solution of 4-hydroxybenzenediazonium tetrafluoroborate at a MWCNT electrode (3 scans, $v = 10$ mV $s^{-1}$, MeCN, 0.1 M TBAP). (B) EPR on (a) nonmodified MWCNT, (b) phenol-modified MWCNT and (c) phenol-modified MWCNT electrodes in the presence of laccase and DMPO in acetate buffer pH 5.5 (90/10 water/DMSO), microwave freq. 9.43 GHz, power 7 mW (a and b) or 2.2 mW (c), mod. amp. 0.3 mT, freq. 100 kHz ($T = 100$ K).

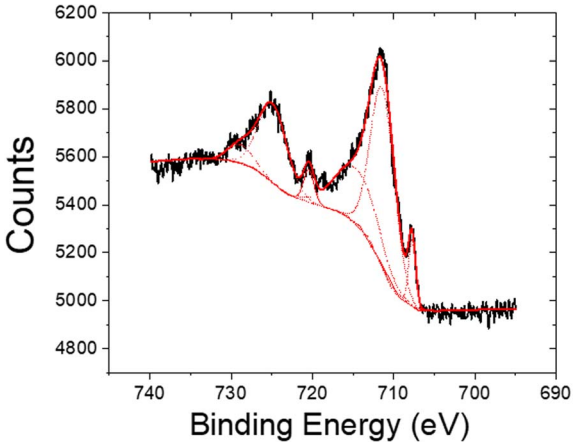


Fig. 5 XPS spectra at the Fe 2p core energy level for the MWCNT electrodes modified with poly-$[Fc^{+}PhO]_n$.

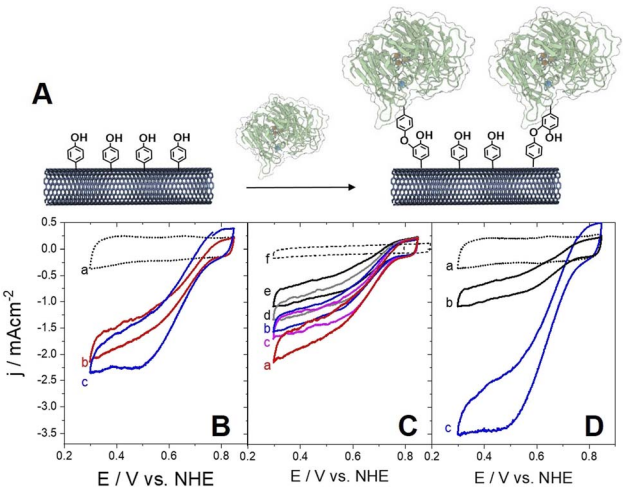


Fig. 6 (A) Schematic representation of the grafting of LAC3 on phenol-functionalized CNTs; (B) CV of phenol-modified MWCNT electrodes after immobilization of LAC3 under (a) Ar, under $O_2$ (b) before and (c) after the addition of 10 mM ABTS (0.05 M acetate buffer solution pH 5, $\nu = 10$ mV $s^{-1}$). (C) CV of phenol-modified MWCNT electrodes after immobilization of LAC3 under $O_2$. Electrodes differ in the number of electrografting cycles: (a) 30 min initial soaking (zero scan), (b) one scan between 0.3 and 0 V, (c) one scan between 0.3 and −0.3 V, (d) three scans between 0.3 and −0.3 V, (e) 5 scans between 0.3 and −0.3 V and (f) non grafted MWCNTs. (D) CV of phenol-modified MWCNT electrodes after immobilization of LAC3 under (a) Ar, under $O_2$ (b) before and (c) after the addition of 10 mM ABTS for a MWCNT electrode modified with 5 scans between 0.3 and −0.3 V (0.05 M acetate buffer solution pH 5, $\nu = 10$ mV $s^{-1}$).

sharp peaks observed at 707.7 and 720.5 eV and corresponding to 4.8% of the total iron content correspond to the presence of Fe(II),[49,57,58] likely trapped in the metallopolymer or adsorbed at the surface of MWCNTs. The broad peaks observed at 711.6 and 725.2 eV, accounting for 96.2% of the iron content are typical of the presence of Fe(III).[57,58] Without the addition of laccase, negligible amounts of ferrocene were detected on the MWCNT surface (Fig. S1†). These results corroborate the enzymatic oxidation and polymerization of poly-$[Fc^{+}PhO]_n$ and its grafting at the surface of MWCNTs.

### Self-grafting of laccase for direct bioelectrocatalytic oxygen reduction

The surface of different proteins is known to be susceptible to covalent modification in the presence of radicals.[59,60] In principle this property could be used for immobilization purpose. Moreover, for a radical-generating enzyme like laccase, immobilization could proceed through a self-catalyzed reaction. The immobilization of the laccase and the direct electrocatalytic reduction of $O_2$ were investigated at phenol-modified MWCNT electrodes. CVs were recorded under saturated $O_2$ purging for phenol-modified MWCNTs ($[O_2] = 0.72$ mmol $L^{-1}$). An irreversible electrocatalytic reduction wave was observed under $O_2$ at phenol-modified MWCNT electrodes, corresponding to the electroenzymatic reduction of $O_2$ into $H_2O$ by immobilized LAC3 (Fig. 6B, curve a). It is noteworthy that LAC3 exhibits poor direct electron transfer (DET) at pristine MWCNT electrodes, which is assessed by negligible electrocatalytic $O_2$ reduction when the enzyme is only adsorbed on MWCNTs (Fig. 6C, curve f).

The influence of the grafting conditions on the final electroenzymatic reduction of $O_2$ was investigated by modulating the initial grafting of the electrode using cyclic voltammetry (electrografting). Actually, best performances – a maximum current density of 1.95 mA $cm^{-2}$ for the electroenzymatic reduction of $O_2$ – were obtained with electrodes for which grafting resulted from a simple soaking of the MWCNT electrodes in a solution of the phenol–diazonium salt for 30 min (Fig. 6C, curve a). Spontaneous grafting of aryl radicals has been shown to be highly efficient at CNT sidewalls.[11,48,51,61,62] We previously demonstrated that spontaneous grafting generates thin layers of polyphenylene, which is favorable for both immobilization of the enzyme and efficient electron tunneling.[11,51,62,63] When higher number of CV scans are performed during electrografting (Fig. 6C, curves b–e) a thicker polyphenylene layer forms and the direct electrocatalytic current density (*i.e.* that promoted by the enzyme) diminishes down to 0.92 mA $cm^{-2}$. This is imputable to the insulating character of the polyphenylene layer that increases the tunneling distance between the electrode and the enzyme electron entry point. In laccases this entry point has been assessed in most cases to be the T1 mononuclear centre but there are reports indicating that the TNC is probably directly accessible from the surface of laccases such as in LAC3.[18,64] Furthermore, electrocatalytic current densities were also assessed in the presence of ABTS, a typical redox partner and mediator of laccases. For thin layers of grafted phenols, the difference in electrocatalytic current densities observed in the presence of ABTS is negligible, underlining that nearly 100% of the enzymes are directly wired (Fig. 6B, curves c *vs.* b).[65] For thick layers of polyphenylenephenol, DET is less efficient and a substantial increase of $O_2$ electrocatalytic current density up to 3.2 mA $cm^{-2}$ is observed in the presence of the mediator (Fig. 6D, curves c *vs.* b). Thus, although a higher number of laccases are immobilized at the thicker phenol layer, not all of immobilized laccases contribute to the DET. This relation between the electrografted layer and the enzyme-mediated current densities was previously observed with LAC3 variants immobilized *via* electrografting and click chemistry

Table 1 Electrochemical characteristics of LAC3 immobilized on MWCNT electrodes *via* noncovalent and covalent strategies *via* direct (DET) or mediated electron transfer (MET)

| LAC3-modified MWCNT electrodes | $I_{max}$ by DET (mA cm$^{-2}$) | $I_{max}$ by MET (ABTS in solution) (mA cm$^{-2}$) |
|---|---|---|
| Pyrene-modified LAC3 (ref. 23) | 1.15 | 2.8 |
| Alkyne-modified LAC3 (ref. 18) | 1.76 | 5.9 |
| This work | 1.95 | 3.2 |



at similar MWCNT electrodes.[18] Actually, oxygen reduction electrocatalysis performances of these newly constructed laccase–phenol-electrodes compare well to our previous work on oriented immobilization of LAC3 and its single lysine variants using noncovalent or covalent strategies (Table 1).[18,23,32] More globally, these biocathodes are as efficient as most biocathodes based on laccases or bilirubin oxidases integrated in enzymatic hydrogen[51,62,66–68] and glucose[4,69,70] fuel cells.

With electrodes constructed with MWCNTs and pyrene-modified LAC3 mutants, we have reached a current density of 1.15 mA cm$^{-2}$ at the same potential. The high performance towards oxygen reduction of the laccase–phenol electrodes is in line with that of our previous electrodes constructed with the same laccase immobilized by the click reaction (such as copper and oxime ligation).[18,32] So, independent of the chemical reactions involved (*i.e.* copper and oxime ligation or phenoxy radical coupling), the bioelectrodes we constructed with the aim of binding the enzyme covalently are comparably both highly efficient. In the case of the laccase–phenol electrode we hypothesize that a DET occurs because of LAC3's ability to oxidize grafted phenol groups and bind to MWCNTs *via* a radical coupling (Fig. 6A). The fact that no phenoxyl radicals originating from grafted phenols are detected at the surface of MWCNTs by EPR (Fig. 3B, curve c) could account for a rapid recombination of the radicals with amino acids located at the laccase's surface. Laccases are able to promote a cross-link probably *via* the oxidation of surface exposed tyrosine residues of different proteins.[71,72] On the other hand, oxidizable tyrosine or tryptophan residues could possibly form a redox chain connecting the TNC to the surface of laccase likely participating in the protection of the TNC from oxidative damage.[73,74] Therefore, surface exposed tyrosine and/or tryptophan could be the residues involved in the coupling of enzymes at phenol-modified MWCNT electrodes. Electroactive layers of the poly-[FcPhO] metallopolymer as well as the highly-efficient direct bioelectrocatalytic reduction of $O_2$ by laccase strongly support the possibility to graft such macromolecules owing to the generation of phenoxy radicals at the nanostructured (*i.e.* phenol-modified) electrode surface. With the previously reported oxidative degradation of catechol-functionalized carbon nanotubes by a peroxidase,[41] the grafting of phenol-functionalized MWCNTs mediated by a laccase is another example of efficient modulation of CNTs' surface properties by enzymes.

## Conclusions

We reported an unprecedented use of laccase for the "grafting to" strategy of aqueous functionalization of CNTs with polyphenols. We demonstrated the ability of laccase to generate phenol radicals at the vicinity of MWCNT electrode surfaces for the subsequent functionalization of MWCNTs with phenol-modified redox molecules. UV-visible spectroscopy, electrochemistry and XPS underline the dual role of laccase in polymerizing phenol-based redox molecules such as FcPhOH and in inducing the functionalization of phenol-modified nanostructured electrodes. High surface concentration of almost 0.1 μmol cm$^{-2}$ was obtained by performing multilayer deposition of a polyphenoxyl metallopolymer. Furthermore, laccase can also be self-immobilized leading to an efficient direct wiring of the enzyme at phenol-modified MWCNT electrodes. Although they have not been directly detected yet, it is tempting to attribute this efficient grafting to enzymatically-generated radicals, possibly both at the surface of the enzyme and CNT sidewalls. This study shows that laccase is a powerful catalyst in the mild surface immobilization of molecules and macromolecules bearing phenol moieties. Our future work will be devoted to the understanding and optimization of this enzyme-catalyzed surface functionalization strategy and its further extension to other molecules of interest.

## Conflicts of interest

There are no conflicts to declare.

## Acknowledgements

This work was supported by the Labex ARCANE ((ANR-11-LABX-0003-01), the Graduate School of Chemistry, Biology and Health of Univ. Grenoble Alpes CBH-EUR-GS (ANR-17-EURE-0003)). The authors acknowledge support from the plateforme de Chimie NanoBio ICMG UAR 2607 (PCN-ICMG) for providing facilities for mass spectrometry analyses and Plateau Synthese Organique (PSO-DCM). Laure Fort is gratefully acknowledged for MALDI experiments and analysis. Valérie Flaud and Dominique Granier from Institut Charles Gerhardt (University of Montpellier 2) are gratefully acknowledged for XPS analysis. We thank Yolande Charmasson and the plateforme AVB: Analyse et Valorisation de la Biodiversité at AMU for technical support in the production of the recombinant enzyme.

## Notes and references

1 S. M. Jones and E. I. Solomon, *Cell. Mol. Life Sci.*, 2015, **72**, 869–883.
2 P. Giardina, V. Faraco, C. Pezzella, A. Piscitelli, S. Vanhulle and G. Sannia, *Cell. Mol. Life Sci.*, 2010, **67**, 369–385.

 

3 A. Le Goff, M. Holzinger and S. Cosnier, *Cell. Mol. Life Sci.*, 2015, **72**, 941–952.
4 N. Mano and A. de Poulpiquet, *Chem. Rev.*, 2017, **118**, 2392–2468.
5 D. M. Mate and M. Alcalde, *Microb. Biotechnol.*, 2017, **10**, 1457–1467.
6 C. Pezzella, L. Guarino and A. Piscitelli, *Cell. Mol. Life Sci.*, 2015, **72**, 923–940.
7 G. Shumakovich, G. Otrokhov, I. Vasil'eva, D. Pankratov, O. Morozova and A. Yaropolov, *J. Mol. Catal. B: Enzym.*, 2012, **81**, 66–68.
8 G. Shumakovich, V. Kurova, I. Vasil'eva, D. Pankratov, G. Otrokhov, O. Morozova and A. Yaropolov, *J. Mol. Catal. B: Enzym.*, 2012, **77**, 105–110.
9 M.-L. Mattinen, K. Kruus, J. Buchert, J. H. Nielsen, H. J. Andersen and C. L. Steffensen, *FEBS J.*, 2005, **272**, 3640–3650.
10 D. Permana, K. Minamihata, M. Goto and N. Kamiya, *J. Biosci. Bioeng.*, 2018, **126**, 559–566.
11 I. Sorrentino, S. Gentil, Y. Nedellec, S. Cosnier, A. Piscitelli, P. Giardina and A. Le Goff, *ChemElectroChem*, 2019, **6**, 1023–1027.
12 I. Sorrentino, I. Stanzione, Y. Nedellec, A. Piscitelli, P. Giardina and A. Le Goff, *Int. J. Mol. Sci.*, 2020, **21**, 3741.
13 I. Sorrentino, M. Carrière, H. Jamet, I. Stanzione, A. Piscitelli, P. Giardina and A. L. Goff, *Analyst*, 2022, **147**, 897–904.
14 C. Lau, E. R. Adkins, R. P. Ramasamy, H. R. Luckarift, G. R. Johnson and P. Atanassov, *Adv. Energy Mater.*, 2012, **2**, 162–168.
15 N. S. Parimi, Y. Umasankar, P. Atanassov and R. P. Ramasamy, *ACS Catal.*, 2012, **2**, 38–44.
16 A. Klonowska, C. Gaudin, M. Asso, A. Fournel, M. Réglier and T. Tron, *Enzyme Microb. Technol.*, 2005, **36**, 34–41.
17 Y. Mekmouche, S. Zhou, A. M. Cusano, E. Record, A. Lomascolo, V. Robert, A. J. Simaan, P. Rousselot-Pailley, S. Ullah, F. Chaspoul and T. Tron, *J. Biosci. Bioeng.*, 2014, **117**, 25–27.
18 S. Gentil, P. Rousselot-Pailley, F. Sancho, V. Robert, Y. Mekmouche, V. Guallar, T. Tron and A. L. Goff, *Chem.–Eur. J.*, 2020, **26**, 4798–4804.
19 Y. Mekmouche, L. Schneider, P. Rousselot-Pailley, B. Faure, A. J. Simaan, C. Bochot, M. Reglier and T. Tron, *Chem. Sci.*, 2015, **6**, 1247–1251.
20 T. Lazarides, I. V. Sazanovich, A. J. Simaan, M. C. Kafentzi, M. Delor, Y. Mekmouche, B. Faure, M. Réglier, J. A. Weinstein, A. G. Coutsolelos and T. Tron, *J. Am. Chem. Soc.*, 2013, **135**, 3095–3103.
21 L. Schneider, Y. Mekmouche, P. Rousselot-Pailley, A. J. Simaan, V. Robert, M. Reglier, A. Aukauloo and T. Tron, *ChemSusChem*, 2015, **8**, 3048–3051.
22 A. J. Simaan, Y. Mekmouche, C. Herrero, P. Moreno, A. Aukauloo, J. A. Delaire, M. Réglier and T. Tron, *Chem.–Eur. J.*, 2011, **17**, 11743–11746.
23 N. Lalaoui, P. Rousselot-Pailley, V. Robert, Y. Mekmouche, R. Villalonga, M. Holzinger, S. Cosnier, T. Tron and A. Le Goff, *ACS Catal.*, 2016, **6**, 1894–1900.
24 A. Le Goff and M. Holzinger, *Sustainable Energy Fuels*, 2018, **2**, 2555–2566.
25 G. García-Molina, M. Pita and A. L. De Lacey, in *Novel Catalyst Materials for Bioelectrochemical Systems: Fundamentals and Applications*, American Chemical Society, 2020, vol. 1342, pp. 207–229.
26 M. T. Meredith, M. Minson, D. Hickey, K. Artyushkova, D. T. Glatzhofer and S. D. Minteer, *ACS Catal.*, 2011, **1**, 1683–1690.
27 H. Cui, L. Zhang, D. Söder, X. Tang, M. D. Davari and U. Schwaneberg, *ACS Catal.*, 2021, **11**, 2445–2453.
28 C. Vaz-Dominguez, S. Campuzano, O. Rüdiger, M. Pita, M. Gorbacheva, S. Shleev, V. M. Fernandez and A. L. De Lacey, *Biosens. Bioelectron.*, 2008, **24**, 531–537.
29 M. Delamar, R. Hitmi, J. Pinson and J. M. Saveant, *J. Am. Chem. Soc.*, 1992, **114**, 5883–5884.
30 P. Allongue, M. Delamar, B. Desbat, O. Fagebaume, R. Hitmi, J. Pinson and J.-M. Savéant, *J. Am. Chem. Soc.*, 1997, **119**, 201–207.
31 D. Bélanger and J. Pinson, *Chem. Soc. Rev.*, 2011, **40**, 3995–4048.
32 S. Gentil, C. Pifferi, P. Rousselot-Pailley, T. Tron, O. Renaudet and A. Le Goff, *Langmuir*, 2021, **37**, 1001–1011.
33 C. Gutiérrez-Sánchez, M. Pita, C. Vaz-Domínguez, S. Shleev and A. L. De Lacey, *J. Am. Chem. Soc.*, 2012, **134**, 17212–17220.
34 P. Singh, S. Campidelli, S. Giordani, D. Bonifazi, A. Bianco and M. Prato, *Chem. Soc. Rev.*, 2009, **38**, 2214–2230.
35 D. Tasis, N. Tagmatarchis, A. Bianco and M. Prato, *Chem. Rev.*, 2006, **106**, 1105–1136.
36 J. O. Zoppe, N. C. Ataman, P. Mocny, J. Wang, J. Moraes and H.-A. Klok, *Chem. Rev.*, 2017, **117**, 1105–1318.
37 T. Matrab, J. Chancolon, M. M. L'hermite, J.-N. Rouzaud, G. Deniau, J.-P. Boudou, M. M. Chehimi and M. Delamar, *Colloids Surf., A*, 2006, **287**, 217–221.
38 C. Gautier, I. López and T. Breton, *Mater. Adv.*, 2021, **2**, 2773–2810.
39 B. L. Allen, P. D. Kichambare, P. Gou, I. I. Vlasova, A. A. Kapralov, N. Konduru, V. E. Kagan and A. Star, *Nano Lett.*, 2008, **8**, 3899–3903.
40 B. Ma, C. Martín, R. Kurapati and A. Bianco, *Chem. Soc. Rev.*, 2020, **49**, 6224–6247.
41 A. R. Sureshbabu, R. Kurapati, J. Russier, C. Ménard-Moyon, I. Bartolini, M. Meneghetti, K. Kostarelos and A. Bianco, *Biomaterials*, 2015, **72**, 20–28.
42 G. Modugno, F. Ksar, A. Battigelli, J. Russier, P. Lonchambon, E. Eleto da Silva, C. Ménard-Moyon, B. Soula, A.-M. Galibert, M. Pinault, E. Flahaut, M. Mayne-L'Hermite and A. Bianco, *Carbon*, 2016, **100**, 367–374.
43 C. Zhang, W. Chen and P. J. J. Alvarez, *Environ. Sci. Technol.*, 2014, **48**, 7918–7923.
44 D. X. Flores-Cervantes, H. M. Maes, A. Schäffer, J. Hollender and H.-P. E. Kohler, *Environ. Sci. Technol.*, 2014, **48**, 4826–4834.
45 V. E. Kagan, N. V. Konduru, W. Feng, B. L. Allen, J. Conroy, Y. Volkov, I. I. Vlasova, N. A. Belikova, N. Yanamala, A. Kapralov, Y. Y. Tyurina, J. Shi, E. R. Kisin, A. R. Murray,

J. Franks, D. Stolz, P. Gou, J. Klein-Seetharaman, B. Fadeel, A. Star and A. A. Shvedova, *Nat. Nanotechnol.*, 2010, **5**, 354–359.
46 V. O. Nyamori and M. D. Bala, *Acta Crystallogr., Sect. E: Struct. Rep. Online*, 2008, **64**, m1630.
47 X. Sun, R. Bai, Y. Zhang, Q. Wang, X. Fan, J. Yuan, L. Cui and P. Wang, *Appl. Biochem. Biotechnol.*, 2013, **171**, 1673–1680.
48 N. Nair, W.-J. Kim, M. L. Usrey and M. S. Strano, *J. Am. Chem. Soc.*, 2007, **129**, 3946–3954.
49 A. Le Goff, F. Moggia, N. Debou, P. Jegou, V. Artero, M. Fontecave, B. Jousselme and S. Palacin, *J. Electroanal. Chem.*, 2010, 57–63.
50 S. Gentil, M. Carrière, S. Cosnier, S. Gounel, N. Mano and A. Le Goff, *Chem.–Eur. J.*, 2018, **24**, 8404–8408.
51 S. Gentil, S. M. Che Mansor, H. Jamet, S. Cosnier, C. Cavazza and A. Le Goff, *ACS Catal.*, 2018, **8**, 3957–3964.
52 N. Lalaoui, M. Holzinger, A. Le Goff and S. Cosnier, *Chem.–Eur. J.*, 2016, **22**, 10494–10500.
53 G. Schmidt, S. Gallon, S. Esnouf, J.-P. Bourgoin and P. Chenevier, *Chem.–Eur. J.*, 2009, **15**, 2101–2110.
54 L. Altamura, C. Horvath, S. Rengaraj, A. Rongier, K. Elouarzaki, C. Gondran, A. L. B. Maçon, C. Vendrely, V. Bouchiat, M. Fontecave, D. Mariolle, P. Rannou, A. Le Goff, N. Duraffourg, M. Holzinger and V. Forge, *Nat. Chem.*, 2017, **9**, 157–163.
55 S. Rengaraj, R. Haddad, E. Lojou, N. Duraffourg, M. Holzinger, A. Le Goff and V. Forge, *Angew. Chem., Int. Ed.*, 2017, **56**, 7774–7778.
56 F. Mao, N. Mano and A. Heller, *J. Am. Chem. Soc.*, 2003, **125**, 4951–4957.
57 M. Umaña, D. R. Rolison, R. Nowak, P. Daum and R. W. Murray, *Surf. Sci.*, 1980, **101**, 295–309.
58 D. O. Cowan, J. Park, M. Barber and P. Swift, *J. Chem. Soc. D*, 1971, 1444–1446.
59 A. C. Mot, C. Coman, N. Hadade, G. Damian, R. Silaghi-Dumitrescu and H. Heering, *PLoS One*, 2020, **15**, e0225530.
60 B. Åkerström, G. J. Maghzal, C. C. Winterbourn and A. J. Kettle, *J. Biol. Chem.*, 2007, **282**, 31493–31503.
61 J. L. Bahr and J. M. Tour, *Chem. Mater.*, 2001, 3823–3824.
62 N. Lalaoui, A. de Poulpiquet, R. Haddad, A. Le Goff, M. Holzinger, S. Gounel, M. Mermoux, P. Infossi, N. Mano, E. Lojou and S. Cosnier, *Chem. Commun.*, 2015, **51**, 7447–7450.
63 N. Lalaoui, A. Le Goff, M. Holzinger, M. Mermoux and S. Cosnier, *Chem.–Eur. J.*, 2015, **21**, 3198–3201.
64 M. Dagys, A. Laurynėnas, D. Ratautas, J. Kulys, R. Vidžiūnaitė, M. Talaikis, G. Niaura, L. Marcinkevičienė, R. Meškys and S. Shleev, *Energy Environ. Sci.*, 2017, **10**, 498–502.
65 N. Lalaoui, A. Le Goff, M. Holzinger and S. Cosnier, *Chem.–Eur. J.*, 2015, **21**, 16868–16873.
66 S. Hardt, S. Stapf, D. T. Filmon, J. A. Birrell, O. Rüdiger, V. Fourmond, C. Léger and N. Plumeré, *Nat. Catal.*, 2021, **4**, 251–258.
67 J. Szczesny, J. A. Birrell, F. Conzuelo, W. Lubitz, A. Ruff and W. Schuhmann, *Angew. Chem., Int. Ed.*, 2020, **59**, 16506–16510.
68 K. Monsalve, I. Mazurenko, N. Lalaoui, A. Le Goff, M. Holzinger, P. Infossi, S. Nitsche, J. Y. Lojou, M. T. Giudici-Orticoni and S. Cosnier, *Electrochem. Commun.*, 2015, **60**, 216–220.
69 C. H. Kwon, S.-H. Lee, Y.-B. Choi, J. A. Lee, S. H. Kim, H.-H. Kim, G. M. Spinks, G. G. Wallace, M. D. Lima, M. E. Kozlov, R. H. Baughman and S. J. Kim, *Nat. Commun.*, 2014, **5**, 3928.
70 A. J. Gross, X. Chen, F. Giroud, C. Abreu, A. Le Goff, M. Holzinger and S. Cosnier, *ACS Catal.*, 2017, **7**, 4408–4416.
71 C. L. Steffensen, M. L. Andersen, P. E. Degn and J. H. Nielsen, *J. Agric. Food Chem.*, 2008, **56**, 12002–12010.
72 T. Heck, G. Faccio, M. Richter and L. Thöny-Meyer, *Appl. Microbiol. Biotechnol.*, 2013, **97**, 461–475.
73 A. Gupta, I. Nederlof, S. Sottini, A. W. J. W. Tepper, E. J. J. Groenen, E. A. J. Thomassen and G. W. Canters, *J. Am. Chem. Soc.*, 2012, **134**, 18213–18216.
74 P. J. Kielb, C. Teutloff, R. Bittl, H. B. Gray and J. R. Winkler, *J. Phys. Chem. B*, 2022, **126**, 7943–7949.

 